J Mater Sci: Mater Electron (2021) 32:15707–15717

Fabrication, illumination dependent electrical and photovoltaic properties of Au/BOD-Pyr/n-Si/In schottky diode

Onur Ongun[1], Enis Taşcı[2], Mustafa Emrullahoğlu[3], Ümmühan Akın[4], Nihat Tuğluoğlu[1], and Serkan Eymur[1,*]

[1] *Department of Energy Systems Engineering, Giresun University, Giresun, Turkey*
[2] *Vocational School of Health Services, Giresun University, Giresun, Turkey*
[3] *Department of Photonics, The İzmir Institute of Technology, İzmir, Turkey*
[4] *Department of Physics, Selçuk University, Konya, Turkey*

Received: 26 January 2021
Accepted: 3 May 2021
Published online: 26 May 2021

ABSTRACT

4,4-Difluoro-4-bora-3a,4a-diaza-s-indacene (BODIPY)-based BOD-Pyr compound was synthesized according to the literature and HOMO and LUMO energies of the BOD-Pyr were calculated by DFT/B3LYP/6-311G(d,p) method using on Gaussian 09 W. Au/BOD-Pyr/n-Si/In Schottky diode were fabricated using thermal evaporation and spin coating technique. The electronic and photovoltaic properties of Au/BOD-Pyr/n-Si/In diode have been investigated by current-voltage (*I-V*) measurements at dark and under various illumination intensities. The calculated ideality factor and barrier height of the diode in dark were found to be 2.84 and 0.75 eV, respectively. These parameters were also obtained under 100 mW/cm^2 illumination level as 1.55 and 0.87 eV, respectively. The values of open-circuit voltage and short circuit current density were obtained as 0.26 V and 0.56 mA/cm^2 under the illumination level of 100 mW/cm^2. These all findings suggest that Au/BOD-Pyr/n-Si/In diode can be used as photodiode in optoelectronic applications.

1 Introduction

Due to their technological advantages in optoelectronic applications, the electrical properties of metal-semiconductor (MS) and metal-interface layer-semiconductor (MIS) type Schottky barrier diodes (SBDs) have been studied in detail in recent years [1, 2]. It is well known that organic compounds used as an interfacial layer for MS contacts have allow us to modify electrical parameters of diodes such as an ideality factor (n) and a barrier height (Φ_B) [3, 4]. Many studies have showed that the organic thin layer on the inorganic semiconductor substrate could affect the performance of these diodes owing to a change of the density of interface states, saturation current and resistance of diode [4–16].

Address correspondence to E-mail: serkan.eymur@giresun.edu.tr

https://doi.org/10.1007/s10854-021-06122-y

Recently, organic dyes as a semiconducting compound have become an exciting area for their use in molecular optoelectronic devices. The most important advantages of organic dyes are their tunable electronic and easy processing features such as high optical and thermal stability, the compatibility with flexible substrates, low cost and easy production in large area applications. Especially, the chemical tunability of organic dyes makes them more promising candidates for modifying charge transport mechanism and band gap and properties. The implementation of organic dyes as semiconductor has been widely used in the fabrication of several optoelectronic devices such as Schottky diodes, photodiodes, organic light-emitting diodes, and solar cells [6, 7, 9, 17, 18].

4,4-Difluoro-4-bora-3a,4a-diaza-s-indacene (BODIPY)-based dyes have gained a great deal of attention in last decades in very diverse applications due to their good favorable chemical, photonic and electronic properties, including easy synthetic functionalization, high photochemical stability, high molar extinction coefficients and high fluorescence quantum yield. These advantages make BODIPY an excellent candidate for use in electronic and optoelectronic devices [19–21]. Nevertheless, compared to considerable interest in outstanding properties of BODIPY dyes, there are only a few studies have made to characterize the electronic parameters of different Schottky diodes which were fabricates by forming BODIPY organic layer on ohmic contact. For example, Kılıcoglu and Ocak measured the ideality factor, barrier height and interface state density of the Phenyl-BODIPY/n-Si structure by current-voltage and capacitance-voltage-frequency techniques [22]. Ozcan et al. fabricated the Al/Subphthalocyanine-BODIPY dyads/p-Si/Al diodes and photoelectrical properties of these diodes was investigated at solar light illuminations [18]. Therefore, further electrical and optical characterizations to investigate π-extended BODIPY compounds are highly desired to show their full potential in different optoelectronic applications.

The main aim of this study is to examine the effect of π-conjugated BODIPY interlayer on the electrical and photoelectrical characteristics of the Au/n-Si diode. For this aim, a π-conjugated BODIPY compound (BOD-Pyr) was synthesized according to published procedure. Then, Au/BOD-Pyr/n-Si/In diode was fabricated to investigate the illumination dependent electrical and photoelectrical properties. These properties were explored by current-voltage measurements.

2 Experimental details

BOD-Pyr was prepared according to published literature procedures [23]. The synthetic route of BOD-Pyr is shown in Scheme 1. First, compound **3** was synthesized from the reaction of benzoyl chloride (**1**) and 2,4-dimethylpyrrole (**2**) in the presence of Et_3N and BF_3.-Et_2O. Then, a Vilsmeier Haack's formylation reaction of compound **3** gave compound **4**. Lastly, Wittig olefination of compound **4** using ylide **5** gave entirely the E-isomer of the BOD-Pyr. The structure of BOD-Pyr was confirmed by ^{1} H, and ^{13} C NMR spectroscopy [23].

The ground state optimize molecular geometry at the gas phase of the isolated compound was obtained with the DFT/B3LYP/6-311G(d,p) computational level within the Gaussian 09 W program [24]. Using this optimized molecular structure, the GaussView5 [25] graphical interface software was used to form the highest occupied molecular orbital (HOMO) and lowest unoccupied molecular orbital (LUMO) simulations. The graphical presentation of HOMO, LUMO orbitals and orbital energy levels are shown in Fig. 1. As seen in Fig. 1, the energy difference between HOMO and LUMO levels (ΔE_g) is 2.73 eV. According to the literature, it is known that the range for ΔE_g is 0.5 to 3.5 eV for semiconductors [26]. The calculated ΔE_g value (2.73 eV) of BOD-Pyr indicates that BOD-Pyr can have a semiconducting behavior.

The Au/BOD-Pyr/n-Si/In diode was constructed using a n-type Si (100) wafer which has 20 Ω.cm resistivity and 500 μm thickness. Then, the solution was stirred for 1 h at ambient temperature. Ultrasonic bath was used to clean n-Si wafer using acetone, methanol and deionized water. Then, the impurities and the native oxide layer on the surfaces were removed using a HF:H_2O (1:10) solution. Ohmic contact was prepared on the back of the n-Si wafer by thermal evaporating of indium metal, and then the wafer was annealed at 350 °C for 30 s in N_2 atmospheres. Then, 10 mg of BOD-Pyr compound was dissolved in 1 ml chloroform. Thin films of BOD-Pyr were made by spin coating at 1200 rpm and 30 s. A satisfactory adherence of the BOD-Pyr film on the n-Si substrate was observed followed by rectifying contacts were deposited. Finally, the front Au contact was

Scheme 1 Synthetic pathway of BOD-Pyr

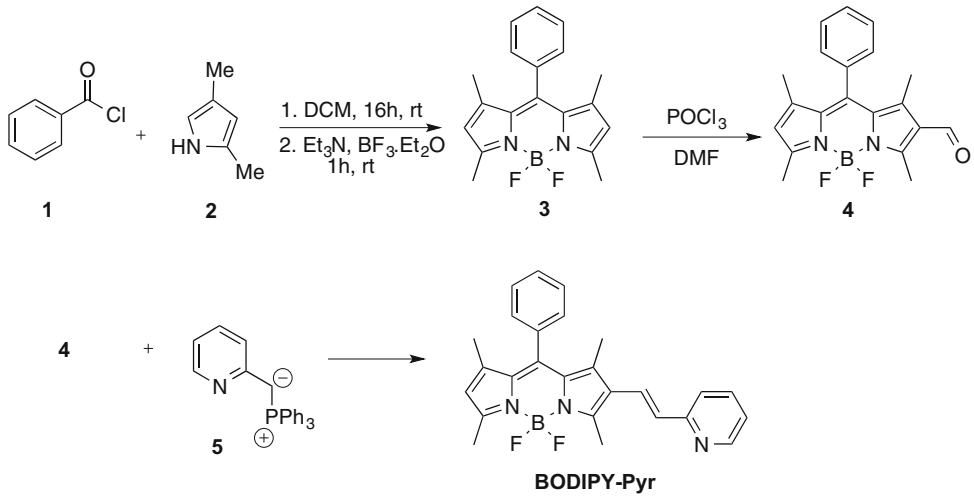

Fig. 1 3D frontier molecular orbital schemes for BOD-Pyr

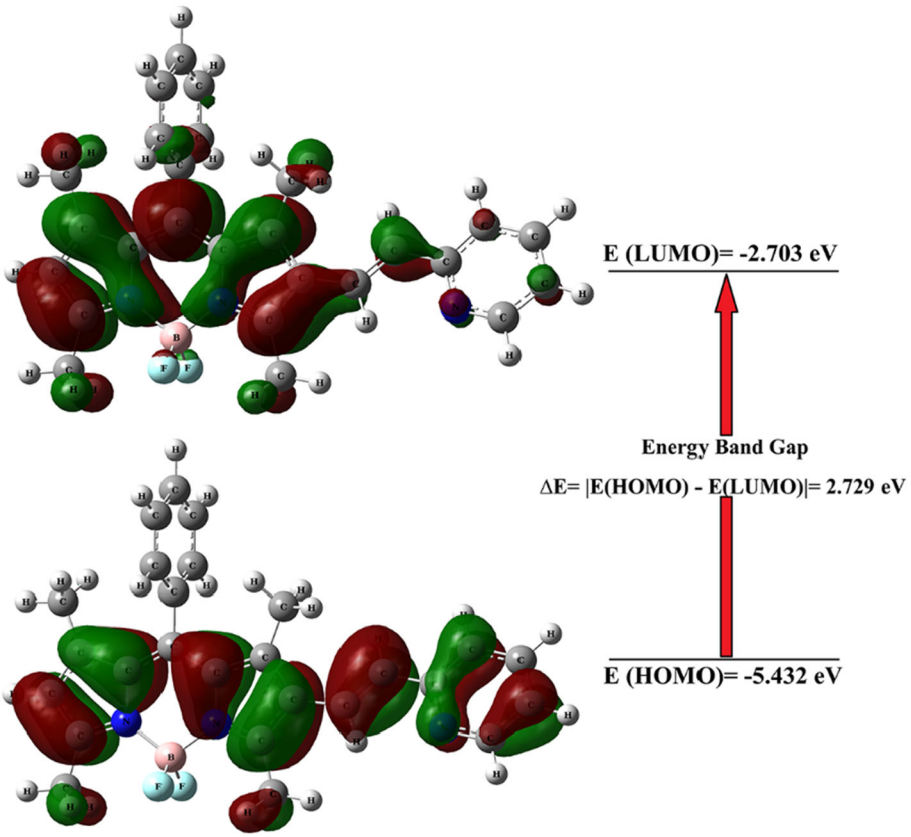

formed on the BOD-Pyr thin film by thermal evaporating as a metallic contact and Au/BOD-Pyr/n-Si/In diode design completed as given in Fig. 2.

3 Results and discussion

The forward and reverse bias *I-V* characteristics of the Au/BOD-Pyr/n-Si/In diode were examined to obtain the junction parameters. The semi-logarithmic *I-V* data for diode were taken in the dark at room

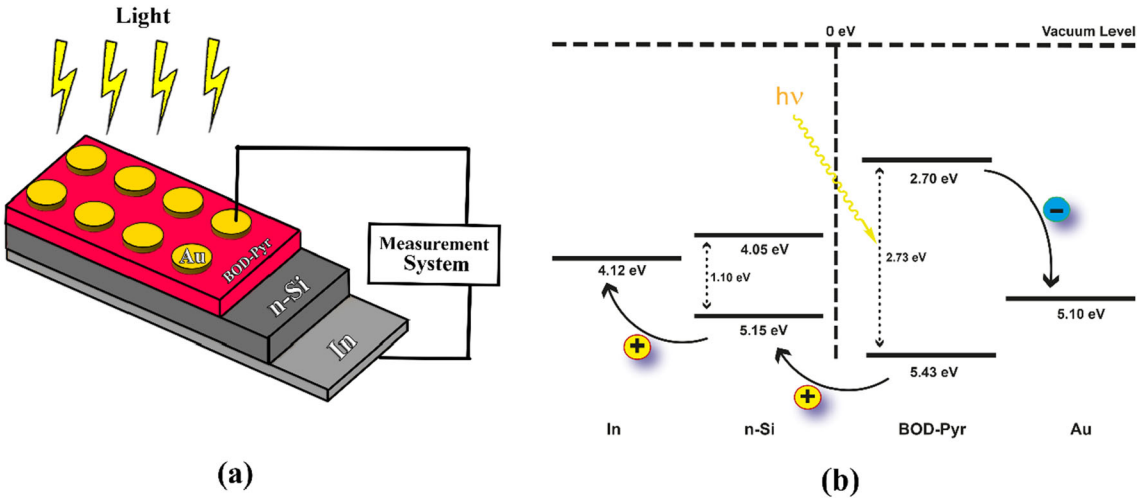

Fig. 2 **a** Schematic diagram of the Au/BOD-Pyr/n-Si/In diode; **b** Schematic energy level diagrams for Au/BOD-Pyr/n-Si/In diode

temperature and under various illumination intensity (20–100 mW/cm^2). As clearly seen in Fig. 3, the Au/BOD-Pyr/n-Si/In diode shows good rectification behavior in the dark. It was calculated that the rectification ratio of the structure at ± 2 V was 100. Thus, thermionic emission theory can be used to obtain diode characteristics [2, 27]. According to Fig. 3, the forward bias semi-logarithmic *I-V* characteristics in dark and under various illumination intensities exhibits two different linear regions with distinct slopes in low voltages ($0.08 < V < 0.20$ in dark and $0.23 < V < 0.30$ in light) and in mid-level voltages ($0.4 < V < 1.1$) which are called as regions I and II, respectively. The relation between *I* and *V* for non-ideal Schottky diodes ($V > 3kT/q$) with a series resistance for two linear regions in dark and under different illumination intensities is expressed according to the thermionic emission (TE) theory as follows [2, 27]:

$$I = I_{01}\left[\exp\left(\frac{q(V\text{-}IR_S)}{n_1kT}\right)\text{-}1\right] + I_{02}\left[\exp\left(\frac{q(V\text{-}IR_s)}{n_2kT}\right)\text{-}1\right] \quad (1)$$

where n_1, n_2, T, q, V and k are defined as ideality factor for regions I and II, temperature in Kelvin, electron charge, applied voltage and Boltzmann constant, respectively. I_{01} and I_{02}defined as the reverse saturation currents for regions I and II are given as,

$$I_{01} = AA^*T^2\exp\left[-\frac{q\Phi B01}{kT}\right] \quad (2)$$

$$I_{02} = AA^*T^2\exp\left[-\frac{q\Phi B02}{kT}\right] \quad (3)$$

where A^* and A are characterized as Richardson coefficient (112 A/cm^{2}K^2 for n-type Si) and effective diode area ($A = 3.14 \times 10^{-2}$ cm^2), respectively. The Φ_B is the zero-bias barrier height which is determined by the following equation:

$$\Phi_B = \frac{kT}{q}\ln\left(\frac{AA^*T^2}{I_0}\right) \quad (4)$$

The ideality factor value can be calculated from the slope of the linear region of the forward bias ln *I-V* characteristics by the following relation:

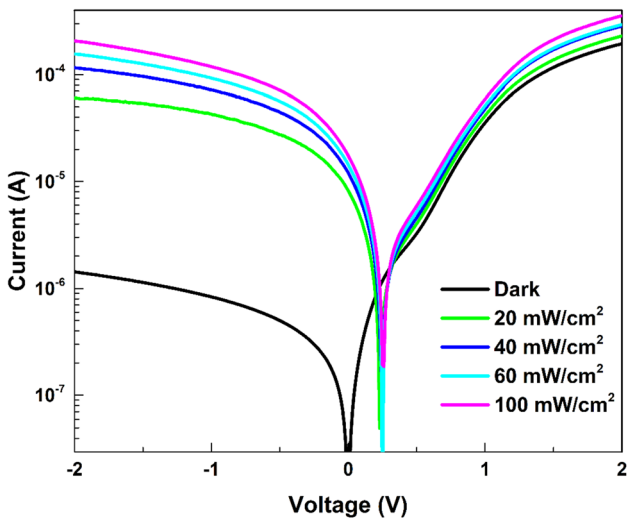

Fig. 3 Experimental forward and reverse *I-V* characteristics of Au/BOD-Pyr/n-Si/In diode

$$n = \frac{q}{kT}\frac{dV}{d\ln(I)} \quad (5)$$

As can be seen in Fig. 3, the current value in reverse bias increases with increasing light intensity and this shows that Au/BOD-Pyr/n-Si/In diode is highly light sensitive and the diode exhibits photovoltaic behavior. The n, Φ_{B0} and I_0 values for dark and under different illumination conditions calculated using I-V plots and Eqs. (1)–(5) for regions I and II are given in Table 1. The Φ_{B0} and n values were computed to be 0.752 − 0.711 eV and 2.84–8.47 in dark, respectively. Also, the Φ_{B0} and n values were computed to be 0.871 − 0.692 eV and 1.55–8.83 under 100 mW/cm^2 illumination level, respectively. The attained n values are greater than unity which may be attributed to factors such as presence of interfacial layer, inhomogeneities of the barrier height, shunt and series resistances, leakage currents and/or a probability of the occurrence of interface states. [28–31]. Also, the high value of n determined for the sample is possibly due to the presence of interfacial states at the heterojunction, which further implies that the thermionic emission is not the only dominating charge carrier transport mechanism [32]; however, there exist some other conduction mechanisms as well. Additionally, high values of ideality factors are referred to secondary mechanisms which contain interface dipoles due to fabrication-induced defects at the interface as well as interface doping or specific interface structure [33, 34].

One of the important parameters that allows us to understand the electrical properties of the diode is series resistance. Using dV/d ln(I) and H(I) functions introduced by Cheung and Cheung [35], as introduced by the Eqs. (6) and (7), it is possible to extract series resistance (R_s) value from the forward biased diode for high voltages.

$$\frac{dV}{d\ln(I)} = \frac{nkT}{q} + IR_s \quad (6)$$

$$H(I) = V - n\frac{kT}{q}\ln\left(\frac{I}{AA*T^2}\right) = n\Phi_B + IR_s \quad (7)$$

First, the dV/d ln(I)-I plots for our sample are given in Fig. 4. According to Fig. 4, plot of dV/d ln(I) versus I will be linear, and its intercept and slope give nand R_s, respectively. The R_s values were computed to be 3.38 kΩ and 1.66 kΩ in dark and under 100 mW/cm^2 illumination level, respectively. Second, the H(I)-I plots for our sample are given in Fig. 5. As can be seen in Fig. 5, plot of H(I) versus I will be linear and its intercept and slope give Φ_B and R_s, respectively. The R_s values were computed to be 3.11 kΩ and 1.30 kΩ in dark and under 100 mW/cm^2 illumination level, respectively. The junction parameters determined from dV/d ln(I) and H(I) plots have been illustrated in Table 2 in dark and under different illumination intensity. The decrease in the value of R_s with the increase of light intensity can be referred to the increase in free carrier concentration by incident light absorption. The decrease in R_s shows that the concentration of free carrier has increased with increasing illumination intensity because the BOD-Pyr layer makes relatively high mobility and ideal charge transport properties. Also, the BOD-Pyr layer may low the function of the oxide layer that may occur on the surface of the silicon by impressing the density distributions of interface states. This confirms that the generation of electron-hole pairs under illumination allows to a decrease the R_s [36]. Furthermore, high R_s values obtained from Cheung's functions can be attributed to the presence of BOD-Pyr interfacial layer between semiconductor and metal and the density of interface states [37]. The high values of the R_s implies that it is a current-limiting factor for the sample [38].

Table 1 Illumination intensity dependent values of n, I_0 and Φ_B obtained from I-V measurements

Illumination intensity (mW/cm^2)	Region I			Region II		
	I_{o1} (A) × 10^{-9}	n_1	Φ_{Bo1} (eV)	I_{o2} (A) × 10^{-7}	n_2	Φ_{Bo2} (eV)
Dark	0.76	2.84	0.75	3.73	8.47	0.71
20	8.14	2.27	0.81	4.90	8.70	0.70
40	4.82	2.08	0.82	5.51	8.65	0.70
60	2.20	1.81	0.84	6.61	8.88	0.69
100	76.6	1.55	0.87	7.43	8.83	0.69

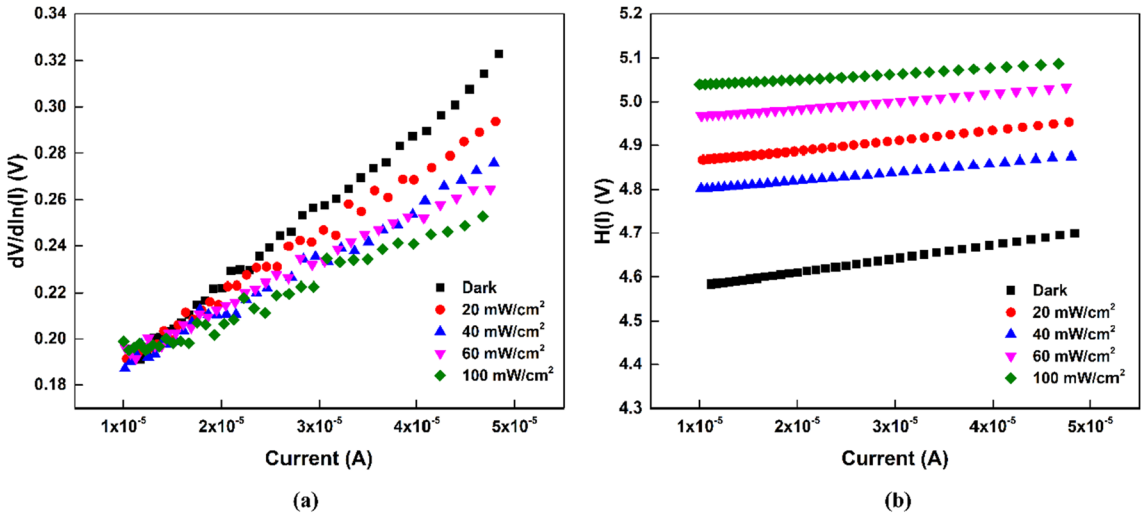

Fig. 4 Illumination dependence of **a** $dV/d\ \ln(I)$ and **b** $H(I)$ versus I for Au/BOD-Pyr/n-Si/In diode

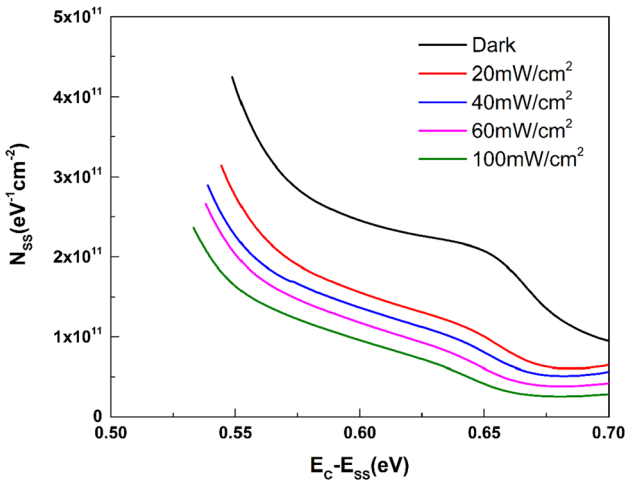

Fig. 5 Illumination intensity dependent N_{ss} against E_c - E_{ss} plots for the Au/BOD-Pyr/n-Si Schottky diode

The interface state density (N_{ss}) in Schottky diodes performs a key role in calculating ideality factor and barrier height. The values of ideality factor (n) against N_{ss} that varies with voltage are introduced by Card and Rhoderick, which is expressed as following relation [39]

$$N_{ss}(V) = \frac{1}{q}\left[\frac{\varepsilon_i}{\delta_i}(n(V)-1) - \frac{\varepsilon_s}{W_D}\right] \tag{8}$$

where ε_s and ε_i are dielectric constant of semiconductor and interface, respectively. The interface layer thickness of organic layer is δ_i and depletion region width is W_D. In n-type semiconductor, the relation of conductivity band limit energy of semiconductor (E_c) with the energy of interface state density (E_{ss}) is expressed by [39].

$$\begin{aligned} E_c - E_{ss} &= q(\Phi_e - V);\ \Phi_e = \Phi_{B0} + \beta V \\ &= \Phi_{B0} + \left(1 - \frac{1}{n(V)}\right)V \end{aligned} \tag{9}$$

where Φ_e is the effective barrier height and q is the electron charge. The variation of interface state density against energy distribution of the Au/BOD-Pyr/n-Si/In Schottky diode at dark and under different illumination intensity is introduced in Fig. 5. As a result of the calculations made according to the plot of Fig. 5, N_{ss} values of Au/BOD-Pyr /n-Si/In

Table 2 Basic electrical parameters of the structure obtained from Cheung's functions

Illumination intensity (mW/cm²)	$dV/d\ \ln(I)$—I		$H(I)$- I	
	R_s (kΩ)	n	R_s (kΩ)	Φ_B (eV)
Dark	3.38	6.18	3.11	0.737
20	2.53	6.67	2.29	0.724
40	2.27	6.87	1.97	0.722
60	2.01	6.92	1.74	0.715
100	1.66	7.02	1.30	0.714

Schottky diode are between 4.25×10^{11} eV^{-1} cm^{-2} for E_c- 0.55 eV and 9.38×10^{10} eV^{-1} cm^{-2} for E_c- 0.70 eV in the dark and also it ranges from 2.36×10^{11} eV^{-1} cm^{-2} for E_c- 0.53 eV to 2.81×10^{10} eV^{-1} cm^{-2} for E_c- 0.70 eV under 100 mW/cm^2 illumination intensity. These energy ranges are higher than the mid-gap of Si. In other words, these states seem to deep-electronic level rather than shallow (donor-type) states. Considering these calculations, it is observed that the increase in the lighting intensity causes a decrease in the interface states. The decreasing values of N_{ss} with the increase in the lighting intensity indicate that the BOD-Pyr interfacial layer acts as passivated material and so lead to fall of the magnitude of N_{ss}. In other words, the use of an organic thin layer between semiconductor and metal has a strong influence on N_{ss} regarding their density distribution and localization in the forbidden gap of semiconductor. Moreover, the decrease of the interface states values can be attributed to the reduction of the free carrier concentration due to trapping of the carriers at the interface. Similar results were obtained by Ersöz et al. [15]. The N_{ss} values of the Au/PPY/n-Si diode fabricated by Ersöz et al. are between 1.7×10^{13} eV^{-1} cm^{-2} and 6.0×10^{12} eV^{-1} cm^{-2} for dark and range from 1.5×10^{13} eV^{-1} cm^{-2} to 4.2×10^{12} eV^{-1} cm^{-2} for 100 mW/cm^2. The N_{ss} values calculated by Ersöz et al. are considerably higher than the values obtained for our sample.

The thickness of the BOD-Pyr interface layer fabricated between the semiconductor and the rectifier contact has been found using the following Eq.

$$C_{org} = \frac{\varepsilon_i \varepsilon_0 A}{d} \tag{10}$$

In the Eq. (10), A is the effective contact area, dis the thickness of the organic interface layer,ε_0 is the permittivity constant of the space and ε_i is the permittivity constant of the interfacial layer. Interfacial organic layer capacitance value (C_{org}) was computed to be 2.41×10^{-10} F from the capacitance value in the accumulation region of 1 MHz *C-V* measurement in Fig. 6. The thickness of the organic interface layer was computed as 3.46×10^{-5} cm (346 nm) from Eq. (10).

The light current density-voltage (*J-V*) curves of the Au/BOD-Pyr/n-Si/In diode are shown in Fig. 7. To understand the photovoltaic performance of diode at different illumination intensities, the basic photovoltaic parameters include open-circuit current voltage (V_{OC}) and short circuit current (J_{SC}) of the diode were analyzed. The V_{OC} value is extracted from the point where the *I-V* curve intersects the voltage axis at this region. The value of J_{SC} is also obtained from the point where the *I-V* curve intersects the current axis at same region. The all obtained values are listed in Table 3. As can be seen, V_{OC} and J_{SC} values have increased while the light intensity increases. This behavior can be considered to be due to an increase in the number of charge carriers by the illumination.

Besides, the values of maximum current (I_m), maximum voltage (V_m) and fill factor (FF) were calculated from Fig. 7 and Eq. (11). The fill factor (FF) is described as follows:

$$FF = \frac{V_m I_m}{V_{oc} I_{sc}} \tag{11}$$

Various conduction mechanisms could be cause for non-ideal forward *I-V* characteristic of Au/BOD-Pyr/n-Si/In Schottky diode. The forward bias *I-V* measurements of Schottky diode for dark are offered in log-log dimension as shown in Fig. 8. As seen in Fig. 8, the characteristic under dark of the sample composed of four linear different areas. The first and second zones are ohmic i.e., the current changes linearly with voltage ($V^{1.1}$ and $V^{1.4}$). These values indicate that the ohmic conduction mechanism is dominant in these zones. The current in third zone depends on voltage as $V^{3.82}$. This shows that the third region is identified trap charge limited current

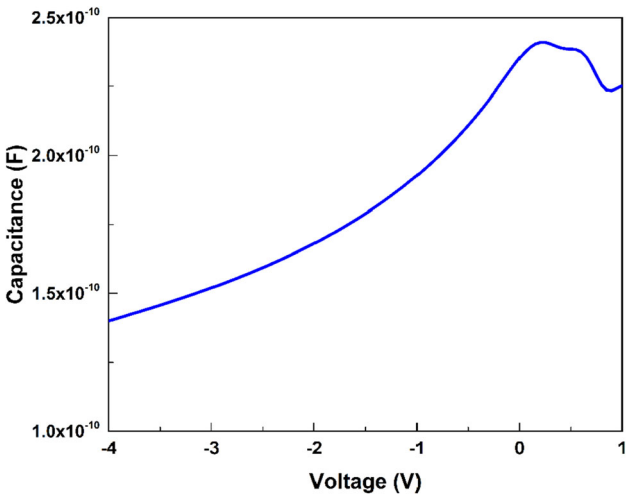

Fig. 6 Capacitance-Voltage plot of Au/BOD-Pyr /n-Si/In Schottky diode at 1 MHz

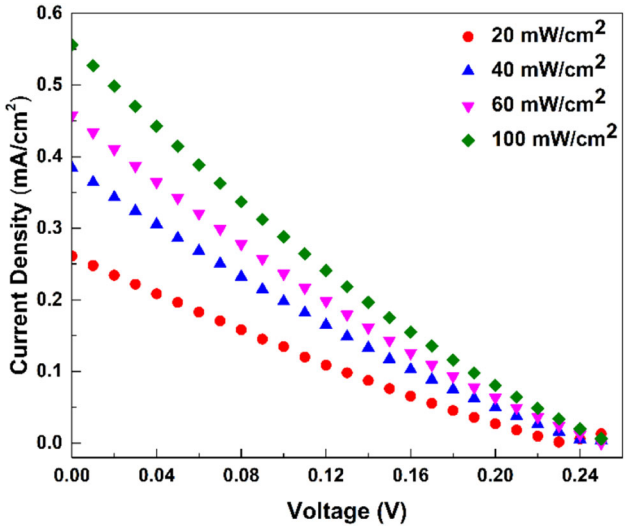

Fig. 7 Current density-voltage (*J-V*) plots of Au/BOD-Pyr/n-Si/In diode under various illumination intensity

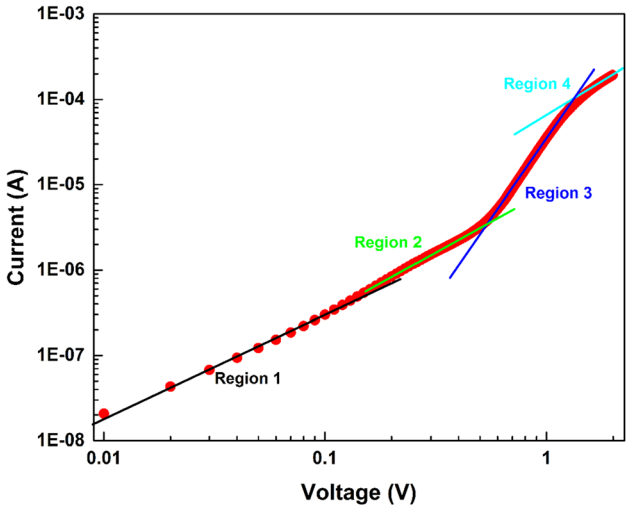

Fig. 8 log (*I*) vs. log (*V*) plot for Al/BOD-Pyr/n-Si Schottky diode at dark condition

(TCLC) mechanism. The current in fourth zone depends on voltage as $V^{2.02}$. This shows that the fourth zone is identified space charge limited current (SCLC) mechanism. Hence, the lower traps are active in this zone and the injected free carriers reason the SCLC conduction mechanism [40–43]. Furthermore, the SCLC conduction technique is generally utilized to identify the characterization of organic Schottky diodes [41, 43, 44].

The photosensitivity (*S*) of the Au/BOD-Pyr/n-Si Schottky diode can be obtained by following Eqs. [45, 46]

$$S(\%) = \left(\frac{I_{photo} 0 I_{dark}}{I_{dark}}\right) \times 100 \quad (12)$$

where I_{photo} and I_{dark} are the photo and dark current, respectively. Figure 9 presents the variation of photosensitivity (*S*(%)) with the illumination intensity (*P*) of our sample at the − 2 V of reverse bias. According to Fig. 9, the photosensitivity *S*(%) value increases with increasing the intensity of illumination. Akın et al. [45] and also Hendi [46] introduced that the reason for the increase in S(%) value is due to the photogenerated charges produced as the electric field increases.

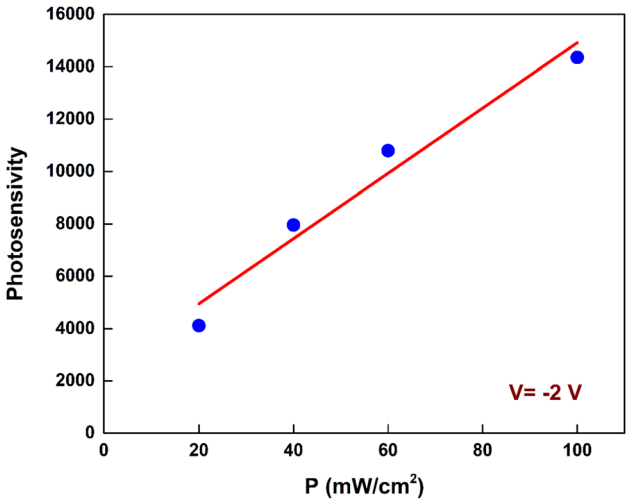

Fig. 9 Plot of photosensitivity vs. *P* of the Au/BOD-Pyr/n-Si Schottky diode

The photoresponsivity (*R*) of the diode is the key parameter to utilize as photodiode. The photoresponsivity (*R*) is expressed according to [45, 46]

Table 3 Illumination intensity dependence of various photovoltaic parameters of Au/BOD-Pyr/n-Si/In diode under various illumination

Power (mW/cm^2)	V_{OC} (V)	J_{SC} (mA/cm^2)	V_m (V)	I_m (mA) x 10^{-7}	FF
20	0.23	0.26	0.10	4.23	22.45
40	0.25	0.38	0.11	6.29	20.84
60	0.25	0.46	0.11	7.50	20.86
100	0.26	0.56	0.11	9.12	20.10

$$R = \frac{I_{photo}}{P.A} \tag{13}$$

where A is the diode area and P is the illumination intensity. The curves of variation of R against V of the Au/BOD-Pyr/n-Si Schottky diode with increasing illumination intensity is illustrated in Fig. 10. As seen, the R values increase with increasing the bias voltage for 20, 40, 60, 100 mW/cm^2. These R values reflect that Au/BOD-Pyr/n-Si Schottky diode can be utilized to fabricate the photodiodes for active applications. These results suggest that the achievement of a n-Si/BOD-Pyr could be characterized as an inorganic/organic photodiode.

The linear variation of the current versus the intensity of illumination is the one of important parameter for a tool to be utilized as a photodiode [40, 45, 47]. The variation of the photocurrent against illumination intensity can be expressed by the following Eqs. [47–49]

$$I_{photo} = \gamma P^{\beta} \tag{14}$$

where γ value is a constant, $\beta$is an exponent which is determined from the slope of the plot and P is the intensity of illumination. Figure 11 presents the curve of $\ln(I_{photo}) - \ln(P)$ for the data of -2 V of Au/BOD-Pyr/n-Si Schottky diode. As can be seen from the curve, these curves present that the photocurrent (I_{photo}) increases as the intensity of illumination increases. The data on this curve present excellent linearity. The value of β describes whether the process of recombination is monomolecular or bimolecular [45]. The β value of our sample was computed as 0.77, which reflects bimolecular recombination mechanism [45, 50]. The β value is also attributed to the trap levels in the gap of energy band [51].

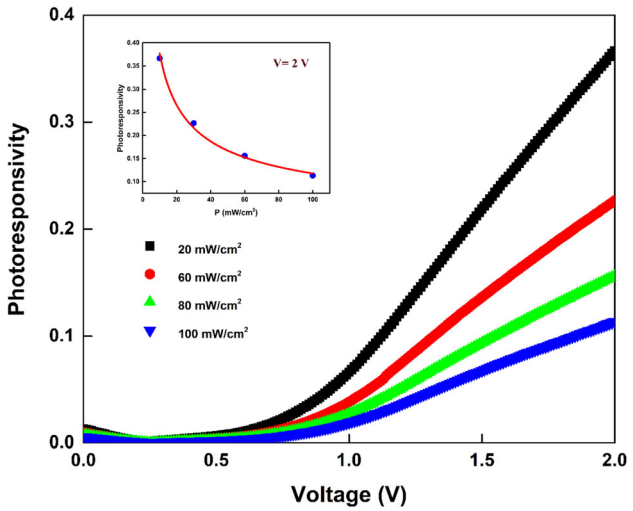

Fig. 10 Plot of photoresponsivity vs. V of the Au/BOD-Pyr/n-Si Schottky diode

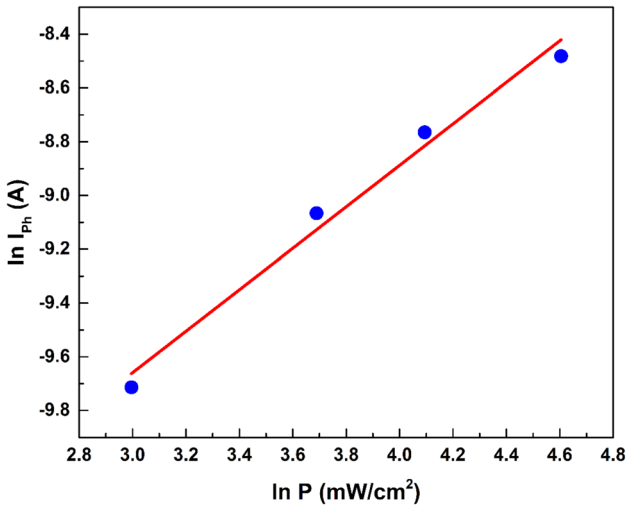

Fig. 11 Plot of $\ln(I_{photo}) - \ln(P)$ of the Au/BOD-Pyr/n-Si at -2 V

4 Conclusions

In this study, Au/BOD-Pyr/n-Si/In diode was produced by coating a BOD-Pyr thin film as an organic interlayer between metal and semiconductor. The electrical and photoelectrical properties were studied in dark and under illumination (20–100 mW/cm^2) using forward and reverse bias I-V measurements. The diode has a high rectification ratio of 100 at dark and ± 2 V. Moreover, it was seen that main diode parameters were strongly dependent upon illumination intensity. The decrease in the ideality factor of the diode and an increase in the barrier height values were observed with the light intensity. The ideality factor and barrier height were found to be 2.84 and 0.75 eV in dark, and 1.55 and 0.87 eV under 100 mW/cm^2 illumination level, respectively. Moreover, the series resistance values obtained by Cheung's method were found in the range of 3.11 kΩ (for dark) – 1.30 kΩ (for 100mW/cm^2). The N_{ss} values have been determined for E_c- 0.70 eV as 9.38×10^{10} and 2.81×10^{10} eV^{-1} cm^{-2} at dark and 100 mW/cm^2 illumination intensity, respectively. The open-circuit voltage and short circuit current density values were found to be as 0.26 V and 0.56 mA/cm^2 under 100

mW/cm^2 illumination level, respectively. Photocurrent (I_{photo}) of the sample increased with increasing the intensity of illumination that reflected bimolecular recombination mechanism. These all findings suggest that Au/BOD-Pyr/n-Si/In diode can be used as photodiode in optoelectronic applications.

Acknowledgements

The authors would like to thank Dr. Halil GÖKCE from Giresun University for his help in discussion of computational studies.

Declarations

Conflict of interest The authors report no declarations of interest.

References

1. E.H. Rhoderick, R.H. Williams, Metal-Semiconductor Contacts, (Clarendon Press Oxford 1988)
2. S.M. Sze, K.K. Ng, *Physics of Semiconductor Devices* (Wiley-Interscience, Hoboken, N.J., 2007)
3. W. Brütting, *Physics of Organic Semiconductors* (Wiley-VCH, Weinheim, 2005)
4. W. Hu, F. Bai, X. Gong, X. Zhan, H. Fu, T. Bjornholm, Organic Optoelectronics, (Wiley-VCH, Weinheim, 2013)
5. J.M. Nunzi, C R Phys. **3**, 523 (2002)
6. A.A.M. Farag, I.S. Yahia, Synth. Met. **161**, 32 (2011)
7. A.G. Imer, E. Kaya, A. Dere, A.G. Al-Sehemi, A.A. Al-Ghamdi et al., J. Mater. Sci.: Mater. Electron. **31**, 14665 (2020)
8. A. Eroğlu, S. Demirezen, Y. Azizian-Kalandaragh, Ş. Altındal, J. Mater. Sci.: Mater. Electron. **31**, 14466 (2020)
9. Y.S. Ocak, M. Kulakci, T. Kilicoglu, R. Turan, K. Akkilic, Synth. Met. **159**, 1603 (2009)
10. O. Güllü, Ş. Aydoğan, A. Türüt, Microelectron. Eng. **85**, 1647 (2008)
11. M.E. Aydın, F. Yakuphanoğlu, J.H. Eom, D.H. Hwang, Phys. B **387**, 239 (2007)
12. T.U. Kampen, S. Park, D.R.T. Zahn, Appl. Surf. Sci. **190**, 461 (2002)
13. O.F. Yüksel, N. Tuğluoğlu, H. Şafak, Z. Nalçacıgil, M. Kuş, S. Karadeniz, Thin Solid Films **534**, 614 (2013)
14. A. Tataroğlu, Ş. Altındal, Y. Azizian-Kalandaragh, J. Mater. Sci.: Mater. Electron. **31**, 11665 (2020)
15. G. Ersöz, I. Yücedağ, S. Bayrakdar, Ş. Altındal, A. Gümüş, J. Mater. Sci.: Mater. Electron. **28**, 6413 (2017)
16. S. Demirezen, H.G. Çetinkaya, M. Kara, F. Yakuphanoğlu, Ş. Altındal, Sens. Actuators A Phys. **317**, 112449 (2021)
17. C. Wang, X. Zhang, W. Hu, Chem. Soc. Rev. **49**, 653 (2020)
18. E. Ozcan, G. Kesan, B. Topaloglu, E.T. Ecik, A. Dere et al., New J. Chem. **42**, 4972 (2018)
19. Y.Q. Fan, J.J. Zhang, Z.Y. Hong, H.Y. Qiu, Y. Li, S.C. Yin, Polymers **13**, 30 (2021)
20. M. Poddar, R. Misra, Coord. Chem. Rev. **421**, 22 (2020)
21. D. Ho, R. Ozdemir, H. Kim, T. Earmme, H. Usta, C. Kim, Chempluschem **84**, 18 (2019)
22. T. Kılıcoğlu, Y.S. Ocak, Microelectron. Eng. **88**, 150 (2011)
23. M. Üçüncü, E. Karakus, M. Emrullahoğlu, New J. Chem. **39**, 8337 (2015)
24. M.J. Frisch, G.W. Trucks, H.B. Schlegel, G.E. Scuseria, M.A. Robb et al., Gaussian 09, Revision C.01, Gaussian Inc, Wallingford, CT, 2009
25. R. Dennington, T. Keith, J. Millam, *GaussView, Version 5, Shawnee Mission KS* (Semichem Inc, 2009)
26. P.W. Atkins, M.E. Hagerman, D.F. Shriver, Inorganic Chemistry, (Oxford Univ. Press, Oxford, 2010)
27. B.L. Sharma, *Metal-Semiconductor Schottky Barrier Junctions and Their Applications* (Springer US, Boston, MA, 1984).
28. J.H. Werner, H.H. Güttler, J. Appl. Phys. **69**, 1522 (1991)
29. R.T. Tung, Mater. Sci. Eng. R Rep. **35**, 1 (2001)
30. M. Ozdemir, D. Choi, G. Kwon, Y. Zorlu, B. Cosut et al., ACS Appl. Mater. Interfaces. **8**, 14077 (2016)
31. R. Kumar, S. Chand, J. Mater. Sci.: Mater. Electron. **25**, 4531 (2014)
32. M. Tahir, M. Ilyas, F. Aziz, M.R. Sarker, M. Zeb et al., Appl. Sci. 10, (2020)
33. G.M. Vanalme, L. Goubert, R.L.V. Meirhaeghe, F. Cardon, P.V. Daele, Semicond. Sci. Technol. **14**, 871 (1999)
34. Ş. Karataş, C. Temirci, M. Çakar, A. Türüt, Appl. Surf. Sci. **252**, 2209 (2006)
35. S.K. Cheung, N.W. Cheung, Appl. Phys. Lett. **49**, 85 (1986)
36. H. Kacuş, M. Yılmaz, A. Koçyiğit, U. İncekara, Ş. Aydoğan, Phys. B **597**, 412408 (2020)
37. U. Aydemir, I. Taşcıoğlu, Ş. Altındal, İ. Uslu, Mater. Sci. Semicond. Process. **16**, 1865 (2013)
38. E. Ugurel, S. Aydogan, K. Serifoglu, A. Turut, Microelectron. Eng. **85**, 2299 (2008)
39. H.C. Card, E.H. Rhoderick, J. Phys. D: Appl. Phys. **4**, 1589 (1971)
40. D.A. Aldemir, M. Benhaliliba, C.E. Benouis, Optik **222**, 10 (2020)
41. I. Ullah, M. Shah, S.A. Khattak, G. Khan, J. Electron. Mater. **48**, 5609 (2019)
42. F. Yakuphanoğlu, N. Tuğluoğlu, S. Karadeniz, Phys. B **392**, 188 (2007)

43. S.Y. Zhu, R.L. Van Meirhaeghe, S. Forment, G.P. Ru, B.Z. Li, Solid·State Electron. **48**, 29 (2004)
44. J. Singh, R.K. Sharma, U.S. Sule, U.K. Goutam, J. Gupta, S.C. Gadkari, Mater. Res. Expr. **4**, 10 (2017)
45. U. Akın, O.F. Yüksel, E. Tascı, N. Tuğluoğlu, Silicon **12**, 1399 (2020)
46. A.A. Hendi, J. Alloys Compd. **647**, 259 (2015)
47. A.G. İmer, A. Dere, A.G. Al-Sehemi, O. Dayan, Z. Serbetci et al., Appl. Phys. A **125**, 10 (2019)
48. E. Elgazzar, O. Dayan, Z. Serbetci, A. Dere, A.G. Al-Sehemi et al., Phys. B **516**, 7 (2017)
49. A.G. İmer, O. Karaduman, F. Yakuphanoğlu, Synth. Met. **221**, 114 (2016)
50. J.G. Simmons, G.W. Taylor, J. Phys. C **7**, 3051 (1974)
51. F. Yakuphanoglu, Microelectron. Reliab. **51**, 2195 (2011)